Available online at www.sciencedirect.com

SciVerse ScienceDirect

Geochimica et Cosmochimica Acta 103 (2013) 301–315

Geochimica et Cosmochimica Acta

www.elsevier.com/locate/gca

Variations of iron flux and organic carbon remineralization in a subterranean estuary caused by inter-annual variations in recharge

Moutusi Roy [a,*], Jonathan B. Martin [a], Jaye E. Cable [b], Christopher G. Smith [c]

[a] Department of Geological Sciences, University of Florida, Gainesville, FL, USA
[b] Department of Marines Sciences, University of North Carolina, Chapel Hill, NC, USA
[c] United States Geological Survey, St. Petersburg, FL, USA

Received 13 June 2012; accepted in revised form 30 October 2012; available online 14 November 2012

Abstract

We determine the inter-annual variations in diagenetic reaction rates of sedimentary iron (Fe) in an east Florida subterranean estuary and evaluate the connection between metal fluxes and recharge to the coastal aquifer. Over the three years study period (from 2004 to 2007), the amount of Fe-oxides reduced at the study site decreased from 192 to 153 g/yr and associated organic carbon (OC) remineralization decreased from 48 to 38 g/yr. These reductions occurred although the Fe-oxide reduction rates remained constant around 1 mg/cm^2/yr. These results suggest that changes in flow rates of submarine groundwater discharge (SGD) related to changes in precipitation may be important to fluxes of the diagenetic reaction products. Rainfall at a weather station approximately 5 km from the field area decreased from 12.6 to 8.4 cm/month from 2004 to 2007. Monthly potential evapotranspiration (PET) calculated from Thornthwaite's method indicated potential evapotranspiration cycled from about 3 cm/month in the winter to about 15 cm/month in the summer so that net annual recharge to the aquifer decreased from 40 cm in 2004 to −10 cm in 2007. Simultaneously with the decrease in recharge of groundwater, freshwater SGD decreased by around 20% and caused the originally 25 m wide freshwater seepage face to decrease in width by about 5 m. The smaller seepage face reduced the area under which Fe-oxides were undergoing reductive dissolution. Consequently, the observed decrease in Fe flux is controlled by hydrology of the subterranean estuary. These results point out the need to better understand linkages between temporal variations in diagenetic reactions and changes in flow within subterranean estuaries in order to accurately constrain their contribution to oceanic fluxes of solutes from subterranean estuaries.
© 2012 Elsevier Ltd. All rights reserved.

1. INTRODUCTION

Iron (Fe) and manganese (Mn) are two important micronutrients that have the potential to control primary productivity in open-ocean and coastal seawater (Sunda et al., 1981; Martin and Fitzwater, 1988; Martin et al., 1994; Hutchins et al., 1998). Two important sources of Fe and Mn to seawater are aerosols (Fung et al., 2000) and solid Fe and Mn phases in continental shelf sediments that dissolve and remobilize during diagenesis (Elrod et al., 2004; Severmann et al., 2010). Recent studies pointed out that an additional source of Fe and Mn to coastal seawater could be dissolved Fe and Mn produced from Fe- and Mn-bearing sediments in subterranean estuaries (e.g., Windom et al., 2006; Roy et al., 2010, 2011, 2012), where sharp geochemical gradients of oxidation potential, pH change, and organic carbon (OC) bioavailability cause dissolution of Fe and Mn oxides and sulfides (Charette and Sholkovitz, 2002; Testa et al., 2002; Spiteri et al., 2006, 2008). Dissolution of Fe and Mn oxides in subterranean estuaries can supply dissolved Fe and Mn with concentrations that are

* Corresponding author.
E-mail addresses: moutusi@ufl.edu (M. Roy), jbmartin@ufl.edu (J.B. Martin).

0016-7037/$ - see front matter © 2012 Elsevier Ltd. All rights reserved.
http://dx.doi.org/10.1016/j.gca.2012.10.055

elevated up to a few 100's μM for Fe and up to about 10 μM for Mn (e.g., Snyder et al., 2004; Beck et al., 2010; Roy et al., 2010).

The term 'subterranean estuary' is given to the underground brackish water zone at the seaward edge of coastal aquifers (Moore, 1999). The portion of the subterranean estuary that is particularly dynamic geochemically is the freshwater discharge zone commonly known as the seepage face, which extends laterally from the shoreline to the freshwater–saltwater boundary (Testa et al., 2002; Charette et al., 2005). Governing hydrological process in the subterranean estuary is submarine groundwater discharge (SGD) (see review by Burnett et al., 2003) originating from both terrestrially derived fresh water (terrestrial freshwater SGD) and saline sea water that circulates through the sediment (marine SGD) (Church, 1996; Moore and Church, 1996; Moore, 2003; Bokuniewicz et al., 2004; Martin et al., 2007; Cable and Martin, 2008). The magnitude of SGD can vary over time, which will affect the position of the freshwater–saltwater boundary (e.g., Herzberg, 1901; Cooper, 1959; Glover, 1964; Fetter, 2001) and change the areal extent of seepage face. Temporal variations in SGD occur at time scales ranging from days (from tides and storms) to months (from seasonal variations in precipitation) to years (from annual to decadal changes in precipitation and sea level rise) (e.g., Taniguchi et al., 2003; Michael et al., 2005; Charette, 2007; Hougham et al., 2008; Smith et al., 2008b; Santos et al., 2009a). Temporal hydrological variations in SGD often result from meteorological conditions, for example, El Niño Southern Oscillation (ENSO) related variations in precipitation (e.g., Anderson and Emanuel, 2008, 2010).

Previous work showed that Fe and Mn oxides dissolution in subterranean estuaries can be enhanced at the freshwater–saltwater boundary (Roy et al., 2011). Consequently, an important question is how temporal variations in SGD may affect rates of Fe and Mn oxide dissolution in seepage faces of subterranean estuaries and thus their fluxes to the oceans. Dissolution rates of Fe and Mn oxide may be expected to increase as flow rates of SGD decrease because of the increase in residence time of groundwater and its capacity to reduce the solid oxide phases. However, in an advection dominated system like subterranean estuaries, where reaction rates are usually orders of magnitude slower than SGD flow rates (Roy et al., 2011), variations in reaction rates may be insufficient to affect the fluxes of the metals. Nonetheless, even with little variation in reactions rates, fluxes of dissolved metals from a subterranean could vary through changes in the width of the seepage face and the volume of sediment in which Fe and Mn oxide dissolution occurs.

In this paper, we evaluate rate variations of Fe-oxide dissolution in the Indian River Lagoon (Florida) seepage face using a set of numerical reactive-transport models of dissolved Fe concentrations, measured during eight sampling trips between 2004 and 2007. Our previous work (e.g., Roy et al., 2010, 2011, 2012) addressed questions related to Fe and Mn dissolution reaction rates at instantaneous moments in time, but did not provide information on how reactions and flow rates vary with time and how these two processes may be linked. We thus address here questions of how reactions rates and fluxes of redox sensitive metals may respond to the inter annual changes in precipitation. Although these changes are known to relate to global weather patterns such as the ENSO, our data records are too short to address changes at a decadal time frame. Nonetheless, we can show that changes in recharge over the three years study period correlate with changes in the fluxes of dissolved Fe from the seepage face. These results demonstrate the critical need to assess temporal variations in diagenetic reactions for estimating fluxes of solutes from subterranean estuaries.

2. LOCATION AND BACKGROUND

Our study site is located in the central Indian River Lagoon near Eau Gallie Creek along the east coast of Florida, U.S.A (Fig. 1). Three hydrostratigraphic units occur in the study area, including from top to bottom the unconfined Surficial Aquifer, confining Hawthorne Group, and confined Floridan Aquifer (Scott, 1988). Because the Floridan Aquifer is confined, all terrestrial SGD originates from the Surficial Aquifer. Three distinct lithostratigraphic units make up the shallow (e.g., <2 m depth) sediments of the subterranean estuary in the study area. These units represent deposition prior to and during the Holocene marine transgression and include, from bottom to top, orange terrestrial sands, grayish-white sands, and black OC-rich marine sands (Hartl, 2006; Roy et al., 2010). Sediment leaching experiments showed that the orange sediments are Fe-oxide coated quartz sands, while the black sediments contain abundant Fe-sulfides, and the intermediate unit has low Fe-oxide and Fe-sulfide contents (Roy et al., 2010).

Porewater Fe maxima occur in the orange Fe-oxide rich sediments, and Fe minima and sulfide maxima occur in the black Fe-sulfide rich sediments. Based on this correspondence between porewater and sedimentary Fe geochemistry, Roy et al. (2010) showed that Fe-sulfide-rich sediments are sinks for dissolved Fe, which is sourced from reductive dissolution of Fe-oxides in the orange sediments. Although the intermediate gray zone lacks Fe-sulfides, Fe isotope data suggested Fe adsorption onto sediments lowers the Fe concentration through this zone (Roy et al., 2012).

The Indian River Lagoon is microtidal, and thus, tides have little effect on the magnitude of terrestrial SGD or the freshwater–saltwater boundary (Smith, 1987; Martin et al., 2007; Smith et al., 2008a,b). This boundary is gradational between fresh and brackish water (with salinity range from 0 to about 25) and the seaward edge of the mixed zone was previously defined as the 300 mM isopleth (Roy et al., 2010, 2011, a value that we adopt here. This boundary was shown to move toward shore by several tens of meters during Tropical Storm Tammy and Hurricane Wilma in 2005 and return to its pre-storm position after 5–7 months (Smith et al., 2008a). During non-storm times, flow rates of terrestrial SGD decrease from 0.16 cm/day at the coastline to no flow at the freshwater–saltwater boundary based on porewater chloride (Cl^-) concentration models (Martin et al., 2007). Flow rates of terrestrial SGD vary seasonally by a factor of nine based on models of radon-222 (^{222}Rn) activity in porewaters (Smith et al., 2008b). The magnitude of terres-

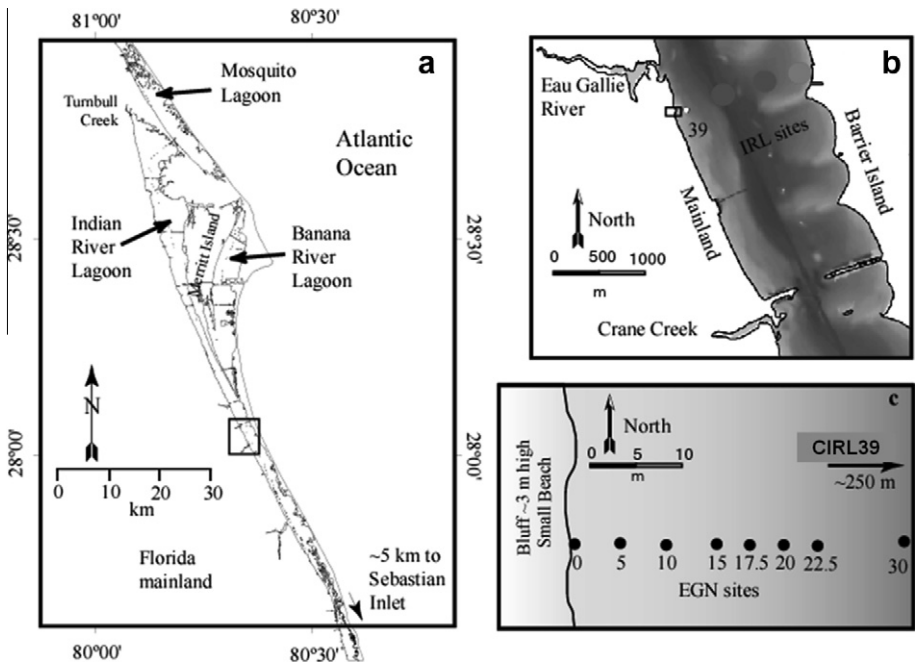

Fig. 1. Description of the study site. (a) Location of the Indian River Lagoon. Small rectangle is the location of inset b. (b) Location of the study site. Small rectangle is the location of inset c. (c) Location of the stations along the transect. Note CIRL 39 is 250 m offshore.

trial SGD correlates inversely with non-local exchange because non-local exchange increases as terrestrial SGD decreases offshore (Martin et al., 2007; Smith et al., 2008a).

Dissolved Fe concentrations vary by several orders of magnitude throughout the subterranean estuary. Porewater Fe concentrations in the Fe-oxide reduction zone increase from less than 1 μM to about 300 μM from the shoreline to the freshwater–saltwater boundary. Roy et al. (2010) suggested elevated dissolved Fe at the freshwater–saltwater boundary is a combination of high Fe-oxide reduction rates at the freshwater–saltwater boundary and the offshore decrease in flow rates of freshwater SGD, which allows dissolved Fe to accumulate at this location.

3. METHODS

3.1. Sample collection and analysis

The study site was a 30 m long shore-perpendicular transect that extended across the seepage face of Indian River Lagoon, Florida (Fig. 1c). The primary sampling sites along the transect are designated as EGNXX, where EGN refers to Eau Gallie North and XX are numbers representing the distance from the shoreline in meters. Porewater samples were collected using multi-level piezometers ("multisamplers"; Martin et al., 2003) at sites EGN0, EGN10, EGN15, EGN17.5, EGN20, and EGN22.5. Two sites, EGN30 and CIRL39, were located offshore of the seepage face. The site CIRL39 (central Indian River Lagoon site 39; Martin et al., 2007) was 250 m offshore and represents the marine background. Multisamplers were installed at EGN0, EGN10, EGN15, and EGN20 in November 2004, and at EGN17.5 and EGN22.5 in February 2005 and May 2005, respectively. Samples were collected in November 2004, February, May, and September 2005, May and October 2006, and April and September 2007 over a period of around 4–6 days for each sampling trip. In October 2006 only a few of the installed multisamplers were sampled (EGN0, EGN20, EGN30, and CIRL39).

Porewaters were collected using a peristaltic pump and filtered through 0.45 μm, trace-metal clean in-line canister type filters (Waterra FHT-45). Dissolved Fe samples were acidified to a pH <2 with ultrapure HNO_3. Dissolved Fe concentrations were measured with an Element-II Inductively Coupled Plasma Mass Spectrometer at the University of Florida (Data are reported in Appendix I). Precision of the measurements was estimated with external standard SLRS4. Repeated measurements ($n = 37$) of the standard yielded Fe concentrations of 1.96 ± 0.07 μm and Mn concentrations of 0.059 ± 0.01 μm, which are within the error range of the certified values of Fe concentrations of 1.84 ± 0.09 μm and Mn concentrations of 0.061 ± 0.003 μm (http://www.nrc-cnrc.gc.ca/obj/inms-ienm/doc/crm-mrc/eng/SLRS-4_e.pdf). Dissolved sulfide concentrations were measured spectrophotometrically in the field immediately following sampling using standard colorimetric techniques (Cline, 1969).

Sediments cores were collected at EGN0, EGN10, EGN20, and EGN22.5 using standard vibracoring techniques, and were analyzed for leachable Fe-oxide concentrations using the technique described by Hall et al. (1996). Sulfur and OC contents of the sediment were measured using a Carlo Erba CNS analyzer. Precision of analysis was estimated for solid phase sulfur (0.1%) and OC (0.016%) based on repeated analyses of in-house standards.

3.2. Reactive-transport model

Details of the reactive-transport model, numerical modeling techniques, model evaluation, and optimization processes were developed and discussed in Roy et al. (2011) and we use those techniques here to model reactions represented in Eqs. (1)–(3) to estimate how Fe and Mn reactions vary over a three year time frame with extreme variations in precipitation. Roy et al. (2011) conceptualized the model domain into three zones: a bottom Fe-oxide dissolution zone (Eq. (1)); an intermediate dissolved Fe adsorption zone (Eq. (2)) and an upper Fe-sulfide precipitation zone (Eq. (3)) (see Fig. 2)

$$C_6H_{12}O_{6(\mathrm{OrgC})} + 42CO_2 + 24Fe(OH)_{3(\mathrm{Fe\text{-}oxide})} \times \xrightarrow{R_1} 24Fe^{2+}_{(\mathrm{Feaq})} + 48HCO_3^- + 18H_2O \quad (1)$$

$$Fe^{2+}_{(\mathrm{Feaq})} \xrightarrow{R_{2b}} Fe_{(\mathrm{adsorbed})} \quad (2)$$

$$Fe^{2+}_{(\mathrm{Feaq})} + HS^- \xrightarrow{R_{2a}} FeS_{(\mathrm{Fe\text{-}sulfide})} + H^+ \quad (3)$$

Because dissolved Fe depth-profiles varied through time, particularly near the freshwater–saltwater boundary, the simple model zonation used by Roy et al. (2011) for data derived from samples collected in April 2004 could not be used to reproduce dissolved Fe profiles from other sampling times. For example, the slope of the dissolved Fe profile changes sharply between the upper and lower part of the Fe-oxide dissolution zone (Fig. 2). We assumed this change in slope within one lithostratigraphic zone indicated variations in rates of Fe-oxides dissolution and divided the Fe-oxide reduction zone into two subzones (Fig. 2). Shallow Fe maxima were observed at EGN20 in November 2004, and in February 2005. These shallow Fe maxima occur near the base of black sediments where the Fe-sulfide content is lower compared to that near the sediment–water interface (Roy et al., 2010). Previous work on geochemical mass transfer (PHREEQC; Parkhurst and Appelo, 1999) modeling showed Fe-sulfide dissolution occurs at the base of the black sediments according to

$$FeS + H_2O \xrightarrow{R_3} FeOH_2 + S^{2-} \quad (4)$$

and we attributed the shallow maximum to this dissolution. Since reactions (3) and (4) occur in different sedimentary zones, both are assumed to be unidirectional i.e. no equilibrium is ever reached between them.

One dimensional reactive-transport equations were formed based on reactions shown as Eqs. (1)–(4). These equations are

$$\frac{\partial C}{\partial t} = D_s \frac{\partial^2 C}{\partial z^2} - \omega \frac{\partial C}{\partial z} + K_1 C_{\mathrm{solid}} \quad (5)$$

$$\frac{\partial C}{\partial t} = D_s \frac{\partial^2 C}{\partial z^2} - \omega \frac{\partial C}{\partial z} - K_2 C \quad (6)$$

where t is time; C is the dissolved Fe concentration; C_{solid} is the Fe-oxide concentration; z is depth below the sediment–water interface (positive downward); ω is the advection rate of terrestrial SGD (negative downward, see Martin et al., 2007); K is a "lumped" rate constant, and D_s is the molecular diffusion coefficient of dissolved Fe, 2.77×10^{-6} cm^2/s (see Roy et al., 2011). These diagenetic equations were numerically solved using MATLAB (The MathWorks, Inc) following Roy et al. (2011).

3.3. Recharge estimates

The monthly recharge to the Surficial Aquifer was calculated from the difference between the monthly average

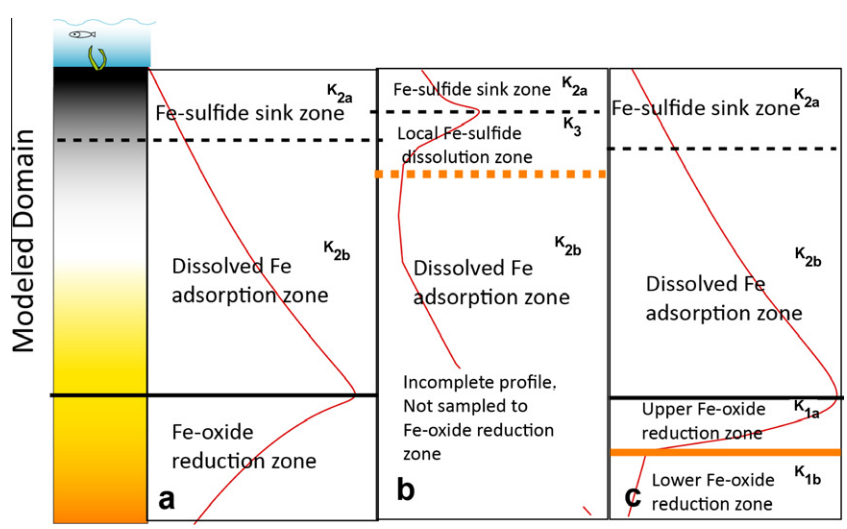

Fig. 2. Conceptual model domains. Three different profiles shapes of dissolved Fe were observed over three years and are shown in panels a, b, and c. The red line represents dissolved Fe profiles, and the left panel represents the corresponding sediment color associated with the three lithostratigraphic units. (a) The black dashed line represents the bottom boundary of Fe-sulfide precipitation zone, and the solid black line represents the boundary between dissolved Fe adsorption zone and Fe-oxide reduction zones (zonation based on samples collected April 2004, see Roy et al., 2011). (b) The zone between black and orange dashed lines represents a local Fe-sulfide dissolution zone, which was not observed in April 2004. (c) The solid orange line separates the upper and lower Fe-oxide reduction zones, which not observed in April 2004). (For interpretation of the references to color in this figure legend, the reader is referred to the web version of this article.)

precipitation and monthly average of evapotranspiration (Appendix II). Monthly precipitation and temperature data were obtained for our study period from National Oceanographic and Atmospheric Administration (NOAA) weather station at the Melbourne Airport, which is within 5 km from the study area (data source: St. John's River Water Management District, Florida, and Southeast Regional Climate Center). The monthly potential evapotranspiration (PET) was calculated from Thornthwaite's method (Thornthwaite and Mather, 1957; Lu et al., 2005; Black, 2007; Eq. (7))

$$E_m = 16N_m\left(\frac{10T_m}{I}\right)^a \quad (7)$$

where, E_m is the monthly PET; N_m is the monthly adjustment factor for the number of daylight hours at our site normalized to 12 h (N_m = daylight hours/12); T_m is the average monthly temperature; I is the annual heat index calculated as the sum of monthly heat index values (i_m), $I = \Sigma i_m$; and a is an exponent based on an empirical relationship for annual heat index, I. The equation to calculate 'i_m' is given by

$$i_m = \left(\frac{T_m}{5}\right)^{1.514} \quad (8)$$

The equation to calculate 'a' is given by

$$a = (6.75 \times 10^{-7} \times I^3) - (7.71 \times 10^{-5} \times I^2) + (1.79 \times 10^{-2} \times I) + 0.49 \quad (9)$$

3.4. ENSO variation and Palmer Z index

The variation in recharge is a weather-related phenomenon that may be linked to global climate variations such as the El Nino Southern Oscillation (ENSO). Variations in ENSO were thus assessed using the Multivariate ENSO Index (MEI) with values available from http://www.esrl.noaa.gov/psd/enso/mei/table.html. Palmer Z index is used as a drought indicator and represents the atmospheric moisture content. The data for Palmer Z index are obtained from http://www.ncdc.noaa.gov/sotc/drought.

4. RESULTS

4.1. Changes in Cl, Fe, and Mn concentrations

From November 2004 to September 2007, the freshwater–saltwater boundary, as estimated by the 300 mM Cl concentration isopleth, moved approximately 5 m landward from about 25 m offshore to around 20 m offshore (Fig. 3). This landward shift appears to be discontinuous, first moving inland by 2.5 m between the September 2005 and May 2006 sampling period and then inland another 2.5 m by October 2006. In April and September 2007, the boundary was constant between 15 and 20 m offshore, but the Cl concentration increased from about 300 mM to greater than 500 mM seaward of the 300 mM Cl isopleth. No such annual changes are observed in the seepage face for dissolved oxygen and pH distributions (data not shown). Dissolved oxygen concentrations were always below 1 mg/L and pH remained approximately neutral during this time.

At all sampling times, zones of elevated Fe and Mn concentrations (dissolved total Fe concentration >100 μM and Mn concentrations >1 μM) were observed at the freshwater–saltwater boundary (Figs. 4 and 5) and these zones moved landward from November 2004 to September 2007 following the freshwater–saltwater boundary. Along with the landward shift in the Cl concentration boundary, the maximum dissolved total Fe concentration at the freshwater–saltwater boundary increased from about 200 μM to about 400 μM and Mn concentration increased from about 2 μM to slightly greater than 3 μM.

4.2. Estimated rate constants and rates of Fe reactions

Distributions of dissolved Fe concentrations and corresponding models for sampling times are shown in Fig. 4. Values are also given for model estimated rate constants for Fe-oxide dissolution and Fe-sulfide precipitation and for fluxes of Fe-oxide driven OC remineralization (Table 1). Dissolved Fe depth profiles have irregular shapes over time so that Fe maxima occur at different depths in the orange sediments and shallow maxima occasionally occur at the base of the black sediments. In general, the rate constants of Fe-sulfide precipitation (K_{2a}) range between 10^{-9} to 10^{-7} mg/cm^2/year. The rate constants of Fe-sulfide precipitation were previously observed to decrease offshore during April 2007 (Roy et al., 2011) and a similar trend is shown here for September 2007. All other sampling periods lack this offshore decrease in rate. The estimated rate constants of Fe-sulfide dissolution (K_3) are orders of magnitude lower than rate constants of Fe-sulfide precipitation (K_{2a}) and generally range between 10^{-12} to 10^{-13} mg/cm^2/year. Overall rates of Fe-sulfide precipitation and Fe-sulfide dissolution show little temporal variation (see Table 1). Modeled rate constants of Fe-oxide dissolution show little variation offshore or through time.

4.3. Annual precipitation change and aquifer recharge

Average monthly precipitation in the study area dropped from about 12.6 cm/month to about 8.4 cm/month from 2004–2005 to 2006–2007 (Fig. 6a). The monthly PET has an annual cycle ranging from around 3 cm/month in the winter to about 15 cm/month in the summer. As a result of the change in precipitation and the seasonality of the PET, the annual recharge to the coastal aquifer dropped from about 40 cm/year to about −10 cm/year from 2004–2005 to 2006–2007 (Fig. 6b). Detailed calculations of recharge estimations and associated evapotranspiration are given in the supplementary data files (see Appendix II). The first 2 years (2004 and 2005) had particularly high amounts of rainfall because of several tropical storms and hurricanes that passed through the region (Smith et al., 2008a), while the last two years had abnormally low rainfall (2006 and 2007), particularly in the typically wet summer and fall.

These changes in precipitation are reflected in the Palmer Z index which shows that seasonal changes controlled

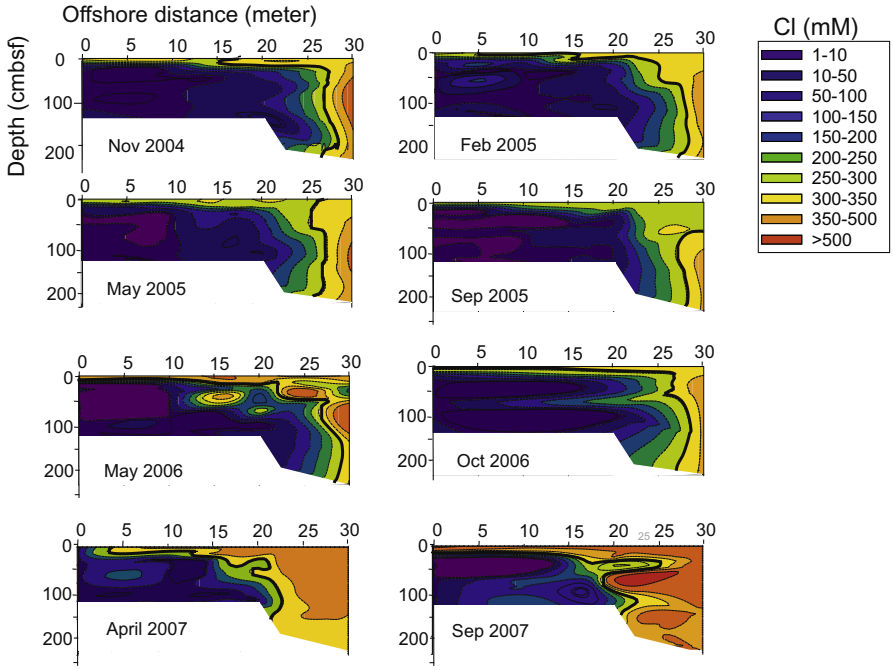

Fig. 3. Temporal variation in Cl concentrations from November 2004 to September 2007. The bold black line in each plot represents the 300 mM Cl concentration isopleth at the time of sampling.

atmospheric moisture content in 2004 and 2005, with moist conditions occurring during the summer rainy season (Fig. 7a). After 2005, the moisture content in the atmosphere became low, with long periods of severe drought and no moist months. These dry periods correspond to the negative MEI values, which occurred twice in the four-year time frame of this study, once from October 2005 to April 2006 and again from March 2007 to September 2007 (Fig. 7b).

5. DISCUSSION

5.1. Fe and Mn geochemistry in subterranean estuaries

Numerous synoptic studies have shown large variations of Fe and Mn concentrations across subterranean estuaries related to geochemical characteristics of the subterranean estuaries (Snyder et al., 2004; Charette et al., 2005; Spiteri et al., 2006, 2008). For example, in the Waquoit Bay subterranean estuary, Massachusetts, dissolved Fe and Mn precipitate as Fe- and Mn-oxide (oxyhydroxide) coatings onto sediment grains, as a result of changes in redox conditions caused by mixing between anoxic freshwater and oxic seawater (Testa et al., 2002; Charette et al., 2005). Within the Waquoit Bay subterranean estuary the oxidation rate of dissolved Fe increases by 7 times from the freshwater to saltwater zone because of an increase in pH values from 5.5 in the freshwater zone to 7.9 in the saltwater zone (Spiteri et al., 2006). In contrast, at Moses Hammock, Georgia, elevated dissolved Fe concentrations are observed at the freshwater–saltwater boundary, because labile DOC concentrations at the boundary enhance Fe-oxide reductions (Snyder et al., 2004). Similar to Moses Hammock, at Waquoit Bay some precipitated Fe-oxides dissolve at the freshwater–saltwater boundary because of high availability of labile dissolved organic carbon (DOC) in porewaters at the boundary (e.g., Charette et al., 2005; Spiteri et al., 2008). These studies reflect the important control of the freshwater–saltwater boundary for Fe and Mn concentrations in the subterranean estuary.

In the Indian River Lagoon subterranean estuary, pH values remain near neutral from the shoreline samples to the freshwater–saltwater boundary and maintain similar depth profiles (Roy et al., 2010). The sedimentary OC (0.04 wt.%) and Fe-oxide (about 0.3 wt.%) contents remain relatively unchanged from the shoreline to the freshwater–saltwater boundary in the orange sediments that represent the Fe-oxide reduction zones (Roy et al., 2010). These relatively invariant OC and Fe-oxide contents and pH conditions result in modeled Fe-oxide reduction rates and
Fe-sulfide precipitation rates that remain within the same order of magnitude from the shoreline to the freshwater–saltwater boundary (see Table 1), unlike the large variations found at Waquoit Bay (Spiteri et al., 2006). Despite the similar reaction rates of Fe across the seepage face, dissolved Fe concentrations increase by three orders of magnitude from the shoreline to the freshwater–saltwater boundary, which Roy et al. (2011) suggested resulted from a decrease in flow rate of terrestrial SGD with distance from the shoreline. Although we do not have models for dissolved Mn, distribution of this trace metal appears to be more sensitive than Fe to the position of the freshwater–saltwater boundary (Fig. 5). Such higher sensitivity

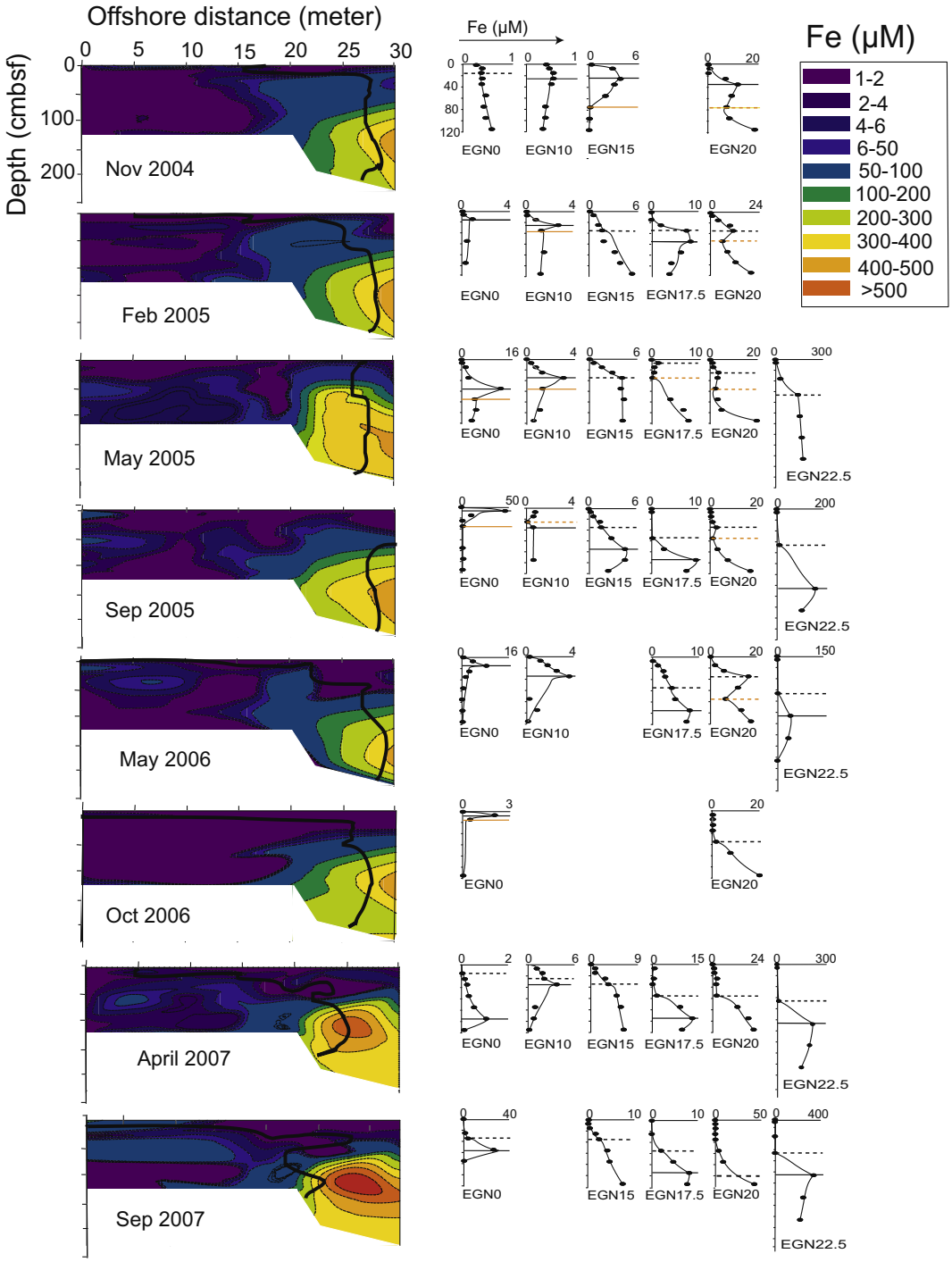

Fig. 4. Temporal variation in distribution of dissolved Fe from November 2004 to September 2007 shown with the 300 mM Cl concentration isopleth (in black) on each plot in the panel on the left. Models of the dissolved Fe concentrations (solid black line) and Fe concentration data (circles) that are used for *in situ* maps are shown in the panel on the right. Note that each panel on the right has a different Fe concentration scale to increase the visual representation of changes in Fe concentration with depth.

of dissolved Mn is expected because reduction of Mn-oxides provides a higher energy yield for microbes and thus is more mobile compared to Fe-oxyhydroxides (e.g., Froelich et al., 1979; McManus et al., 2012).

5.2. Annual variations in Fe and OC fluxes

Fluxes of Fe and OC from the seepage face of the Indian River Lagoon result from terrestrial SGD with little

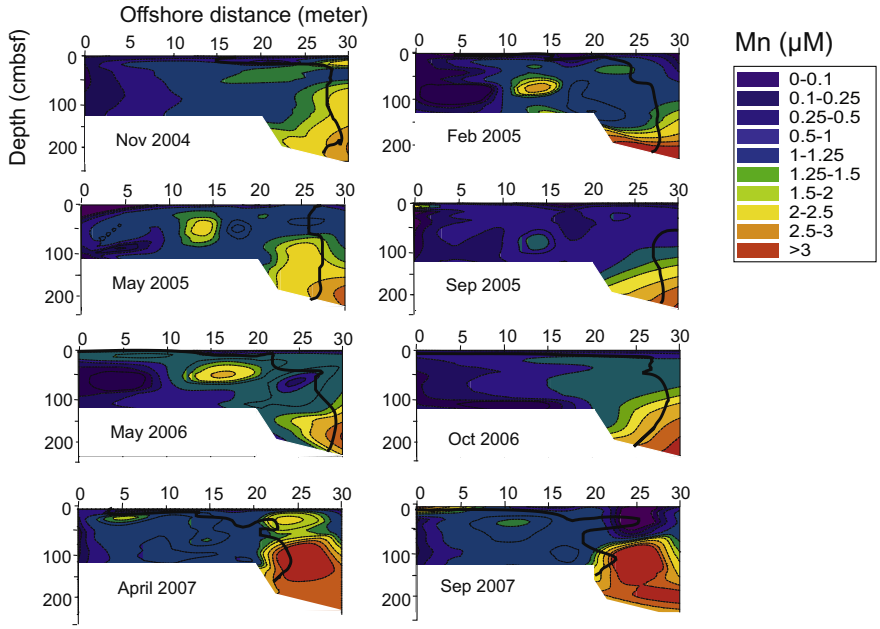

Fig. 5. Temporal variation in distribution of dissolved manganese (Mn) from November 2004 to September 2007 shown with the 300 mM Cl concentration isopleth (in black) overlain on each plot.

influence of non-local exchange because the upward flow of terrestrial SGD limits the depth of non-local exchange within the sediments (Roy et al., 2011). As SGD flows upward through the shallow black lithostratigraphic unit, sulfide minerals precipitate (Eq. (3)) and thus this unit represents a sink for Fe within the seepage face of the subterranean estuary. Iron-sulfide dissolution is not an important source of dissolved Fe concentrations in these sediments because the dissolution rate constants are orders of magnitude lower than rates of Fe-sulfide precipitation. Our model of Fe diagenesis thus ignores the effects of non-local exchange and assumes the black sediments, in general, represent a net sink for dissolved Fe within the seepage face.

Model results show reaction rates of dissolved Fe production are nearly constant, averaging about 1 mg/cm^2/yr, from November 2004 to September 2007 (see Table 1), but the seaward edge of the seepage face decreased from about 25 m in November 2004 to about 20 m in September 2007 (Fig. 3). Considering a 1-m wide strip of the seepage face, the area of the seepage face in the strip decreased by about 20% from 25 to 20 m^2. Multiplying the Fe-oxide dissolution rate by this unit area, we estimate the upward flux of dissolved Fe sourced from the reduction of Fe-oxide coated sediments over 1 m depth interval decreased from 192 to 154 g/yr from November 2004 to September 2007. Much of this Fe is trapped as Fe-sulfides within the black sediments and does not discharge to the lagoon water until seepage face moves offshore following transgression and Fe is remobilized from the Fe-sulfides by non-local exchange (e.g., Roy et al., 2010).

Assuming that all Fe-oxide reduction results from OC remineralization with a stoichiometry of one mole of OC remineralized for every four moles of Fe-oxides reduced (Eq. (1)), the amount of OC remineralization decreased from 48 to 38 g/yr between November 2004 and September 2007. The DIC produced from this OC remineralization may be discharged to the lagoon because it would not be re-precipitated within the Fe-sulfide sediments (Dorsett et al., 2011). Dissolved Fe concentrations increased during the 2007 sampling periods from previous sampling times even though less Fe-oxide was reduced as a result of the smaller seepage face (Fig. 4 and Table 1). The increase in Fe concentrations corresponding to the decrease in the total amount of Fe-oxide reduction in the seepage face suggests dissolved Fe may accumulate at the freshwater–saltwater boundary during the drought year as a result of decreased discharge of terrestrial SGD.

The estimated Fe-oxide reduction and Fe-oxide driven OC oxidation rate constant values at our site (see Table 1) are similar to the DOC oxidation rate used in a similar flow-transport model for Waquoit Bay (Spiteri et al., 2008). At Waquoit Bay, the modeled rate constant was two orders of magnitude higher for labile marine DOC (3.0×10^{-7} s^{-1}) than for terrestrial DOC (3.0×10^{-10} s^{-1}) (Spiteri et al., 2008). These similarities are somewhat surprising considering that multiple differences exist in characteristics of Waquoit Bay and Indian River Lagoon. For example, the major electron acceptor for marine DOC at Waquoit Bay site is NO_3^- and for Indian River Lagoon, where very little NO_3^- is present, is likely Fe-oxides. Waquoit Bay has OC-poor sediments (ranging from about 0.015–0.075 wt.%) compared to Indian River Lagoon (ranging from about 0.04 wt.% to about 0.34 wt.%). The subterranean estuary of Waquoit Bay is suboxic whereas Indian River Lagoon is hypoxic (Charette et al., 2005; Spiteri et al., 2008; Roy et al., 2011). Regardless of these differences, the similar values for OC remineralization rate constants suggest subterranean estuaries are important sites

Table 1
Model results. Blank cells indicate that either zone has not been sampled or dissolved Fe profile shape does not indicate presence of this zone.

K_{1a} (1/s)	Offshore distance (m)					
	0	10	15	17.5	20	22.5
Nov-04		5.98×10^{-14}	2.31×10^{-11}			
Feb-05	2.30×10^{-12}	4.20×10^{-11}		1.84×10^{-12}		–
May-05	3.20×10^{-10}	3.87×10^{-12}				–
Sep-05	8.53×10^{-10}	2.14×10^{-14}	3.03×10^{-12}	3.52×10^{-12}		1.07×10^{-11}
May-06	1.84×10^{-11}	9.06×10^{-13}		1.21×10^{-12}		4.76×10^{-12}
Oct-06	4.32×10^{-12}					–
April-07	3.78×10^{-12}	1.81×10^{-12}		4.99×10^{-12}		8.90×10^{-12}
Sept-07	1.15×10^{-9}			7.50×10^{-13}		4.75×10^{-12}
Average	3.36×10^{-10}	8.11×10^{-12}	1.31×10^{-11}	2.46×10^{-12}		7.28×10^{-11}
K_{1b} (1/s)						
Nov-04			8.74×10^{-14}			
Feb-05		1.17×10^{-13}				
May-05	4.15×10^{-12}	5.11×10^{-13}				
Sep-05	6.77×10^{-13}					
May-06						
Oct-06	3.76×10^{-13}					
April-07						
Sept-07						
Average	1.73×10^{-12}	3.14×10^{-13}	8.74×10^{-14}			
K_{2a} (1/s)						
Nov-04	5.88×10^{-10}	6.71×10^{-9}	6.67×10^{-9}		4.72×10^{-8}	
Feb-05	3.68×10^{-7}	1.53×10^{-7}	1.96×10^{-8}	1.04×10^{-7}	1.93×10^{-8}	
May-05	1.27×10^{-7}	9.21×10^{-8}	3.98×10^{-8}	3.25×10^{-8}	4.31×10^{-8}	1.24×10^{-8}
Sep-05	1.49×10^{-7}		3.15×10^{-8}	1.57×10^{-8}	4.83×10^{-8}	7.82×10^{-9}
May-06	1.96×10^{-7}	4.33×10^{-8}		1.31×10^{-8}	5.71×10^{-8}	
Oct-06	2.68×10^{-7}				5.61×10^{-8}	
April-07	21.9×10^{-8}	2.80×10^{-8}	3.63×10^{-8}	3.91×10^{-8}	2.7×10^{-9}	6.4×10^{-9}
Sept-07	1.86×10^{-7}		5.37×10^{-8}	5.20×10^{-8}	4.55×10^{-8}	1.23×10^{-8}
Average	2.16×10^{-7}	7.91×10^{-8}	3.62×10^{-8}	4.27×10^{-8}	3.89×10^{-8}	9.73×10^{-9}
K_{2b} (1/s)						
Nov-04	9.97×10^{-9}				1.76×10^{-8}	
Feb-05			6.82×10^{-9}	1.24×10^{-9}	9.72×10^{-9}	
May-05			1.33×10^{-10}	1.13×10^{-8}	3.16×10^{-8}	2.72×10^{-10}
Sep-05		1.39×10^{-7}	1.86×10^{-8}	3.88×10^{-8}	1.97×10^{-8}	3.47×10^{-9}
May-06				1.28×10^{-8}	6.50×10^{-9}	3.92×10^{-9}
Oct-06					9.64×10^{-9}	
April-07	5.74×10^{-8}	5.36×10^{-8}	2.9×10^{-9}	1.39×10^{-8}	4.8×10^{-9}	7.6×10^{-8}
Sept-07	1.11×10^{-7}		8.43×10^{-9}	1.67×10^{-8}	1.72×10^{-8}	8.51×10^{-9}
Average	5.95×10^{-8}	9.63×10^{-8}	7.38×10^{-9}	1.58×10^{-8}	1.58×10^{-8}	1.84×10^{-8}
K_3 (1/s)						
Nov-04					2.28×10^{-12}	
Feb-05					5.37×10^{-12}	
May-05				1.33×10^{-13}	7.42×10^{-13}	
Sep-05		2.89×10^{-12}			1.93×10^{-12}	
May-06					7.16×10^{-12}	7.58×10^{-9}
Oct-06						
April-07						
Sept-07						
Average		2.89×10^{-12}		1.33×10^{-13}	3.50×10^{-12}	7.58×10^{-9}
Fe-sulfide precipitation in upper zone (mg/cm^2/year)						
Nov-04	0.00	0.00	0.02		0.19	
Feb-05	0.03	0.10	0.03	0.26	0.17	
May-05	1.68	0.15	0.12	0.00	0.05	3.10
Sep-05	0.23		0.04	0.01	0.08	0.21

(*continued on next page*)

Table 1 (*continued*)

K_{1a} (1/s)	Offshore distance (m)					
	0	10	15	17.5	20	22.5
May-06	0.22	0.13		0.11	0.51	0.03
Oct-06	0.02				0.08	
April-07	0.00	0.03	0.09	0.08	0.02	0.21
Sept-07	0.36		0.08	0.10	0.16	0.01
Average	0.32	0.08	0.06	0.09	0.16	0.71
Fe-adsorption in the intermediate zone (mg/cm^2/year)						
Nov-04	0.06				0.36	
Feb-05			0.21	0.01	0.53	
May-05			0.00	0.37	0.81	0.79
Sep-05			0.00	0.37	0.81	0.79
May-06				0.15	0.22	0.35
Oct-06				0.15	0.22	0.35
April-07	0.18	0.02	0.13	0.22	0.31	2.25
Sept-07	0.85		0.34	0.17	1.37	2.83
Average	0.36	0.02	0.14	0.20	0.58	1.23
Total dissolved Fe-loss (mg/cm^2/year)						
Nov-04	0.06	0.00	0.02		0.55	
Feb-05	0.03	0.10	0.25	0.26	0.70	
May-05	1.68	0.15	0.12	0.37	0.86	3.89
Sep-05	0.23	0.22	0.15	0.29	0.81	2.67
May-06	0.22	0.13		0.26	0.78	0.38
Oct-06	0.02				0.67	
April-07	0.05	0.05	0.22	0.30	0.33	2.46
Sept-07	1.21		0.42	0.27	1.53	2.84
Average	0.44	0.11	0.20	0.29	0.78	2.45
Total Fe-sulfide dissolution (mg/cm^2/year)						
Nov-04					0.08	
Feb-05					0.06	
May-05				0.02	0.02	
Sep-05		0.01			0.02	
May-06					0.28	
Oct-06						
April-07						
Sept-07						
Average		0.01		0.02	0.09	
Total Fe-oxide dissolution (mg/cm^2/year)						
Nov-04		0.02	45.50			
Feb-05	0.68	0.13		0.11		
May-05	0.64	0.13				
Sep-05	1.44	0.14	0.00	0.05		0.90
May-06	5.37	0.25		0.02		0.13
Oct-06						
April-07	0.05	0.48		0.07		0.24
Sept-07	5.12			0.01		0.13
Average	2.22	0.19	22.75	0.05		0.35
OC remineralization by Fe-oxides (mg/cm^2/year)						
Nov-04		0.00	11.38			
Feb-05	0.17	0.03		0.03		
May-05	0.16	0.03				
Sep-05	0.36	0.04	0.00	0.01		0.67
May-06	1.34	0.06		0.00		0.03
Oct-06						
April-07	0.01	0.12		0.02		0.06
Sept-07	1.28			0.07		0.03
Average	0.55	0.05	5.69	0.03		0.20

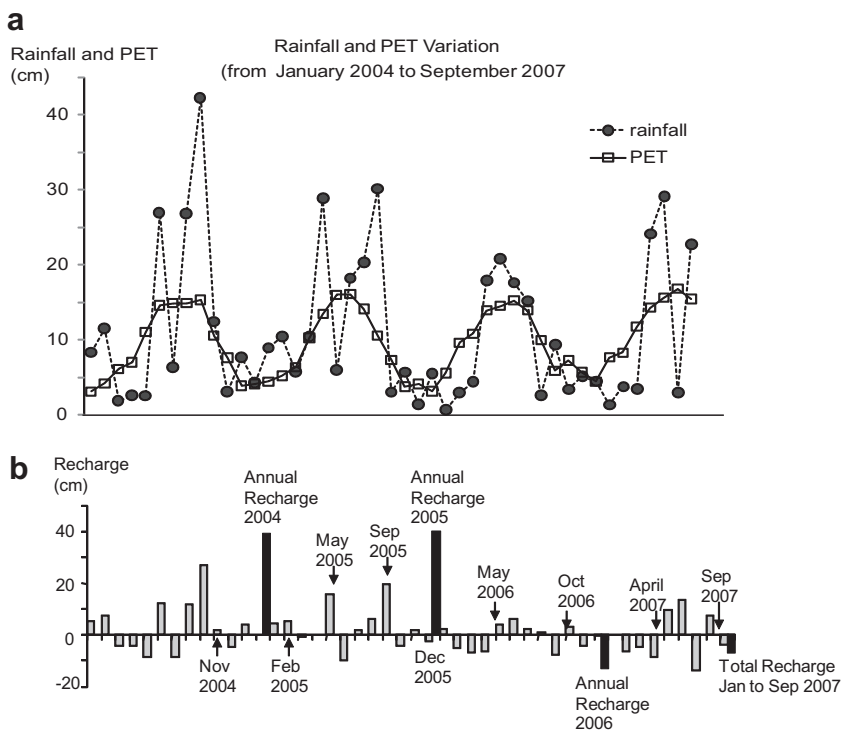

Fig. 6. Temporal variation in rainfall, PET and recharge to the aquifer from January 2004 to September 2007. (a) Variations in rainfall and calculated PET. (b) Variations in aquifer recharge. Light grey bars represent monthly recharge and dark grey bars represent total annual recharge. Sampling times are indicated by small arrows associated with the dates. Note, in 2007 total recharge was calculated from the beginning of January to the end of September (the last time of sampling).

for OC remineralization and possibly to the global C budget. The fact that reaction rate constants are similar from 2004 to 2007 indicates that in an advection dominated system, where reaction rates are orders of magnitude slower than SGD flow rates like Indian River Lagoon (see Roy et al., 2011), fluxes of dissolved metals from subterranean estuary should be controlled mainly by flow.

5.3. Temporal changes in hydrology

Our measurements of Cl concentrations (Fig. 3) do not reflect changes in hydrology at diurnal, episodic, or seasonal time frames. Shifts in the freshwater–saltwater boundary can occur at tidal frequencies in tide-dominated subterranean estuaries (Dulaiova et al., 2006; Burnett et al., 2007; Santos et al., 2009a,b,c), but the lack of diurnal variations in Cl concentrations at Indian River Lagoon subterranean estuary may result from its small (about 10 cm) tidal range (Smith, 1987; Martin et al., 2007). Rapid daily water exchange was observed near the sediment–water interface at site CIRL39 because of bioirrigation, but this exchange is a continuous process and represents a steady state condition beyond the seepage face zone (Martin et al., 2004, 2006; Cable et al., 2006). However, hydrologic changes at episodic and seasonal time frames do occur in Indian River Lagoon and we address these changes below.

5.3.1. Episodic variations in SGD

Storms can move the position of the freshwater–saltwater boundary by several meters over time scales of months in the Indian River Lagoon subterranean estuary. The storm surge caused by Hurricane Wilma (October, 2005) increased the water level of the lagoon above the hydraulic head of the subterranean estuary, pumping lagoon water into the subterranean estuary, causing the freshwater–saltwater boundary to shift landward by approximately 10 m (Smith et al., 2008a). Our sampling time in September 2005 occurred immediately prior to Hurricane Wilma and the subsequent sampling period in May 2006 occurred after the freshwater–saltwater boundary had returned to pre-storm conditions (Smith et al., 2008a). Consequently, our data show little evidence for the shift in Cl concentrations that was observed by Smith et al. (2008a), except for lens-shaped zone of elevated Cl concentrations about 15–20 m offshore and 50 cmbsf in May 2006, suggesting the influx of lagoon water following Hurricane Wilma was not completely flushed by the time of our sampling (Fig. 3). This elevated Cl zone was observed near the seaward edge of the subterranean estuary (Martin et al., 2007) where flow is slow, indicating limited flushing retained the storm signature. No corresponding increase in dissolved Fe and Mn concentrations occurred with the elevated Cl concentrations, however, suggesting that either diagenetic reactions that increased the Fe and Mn concentrations were not

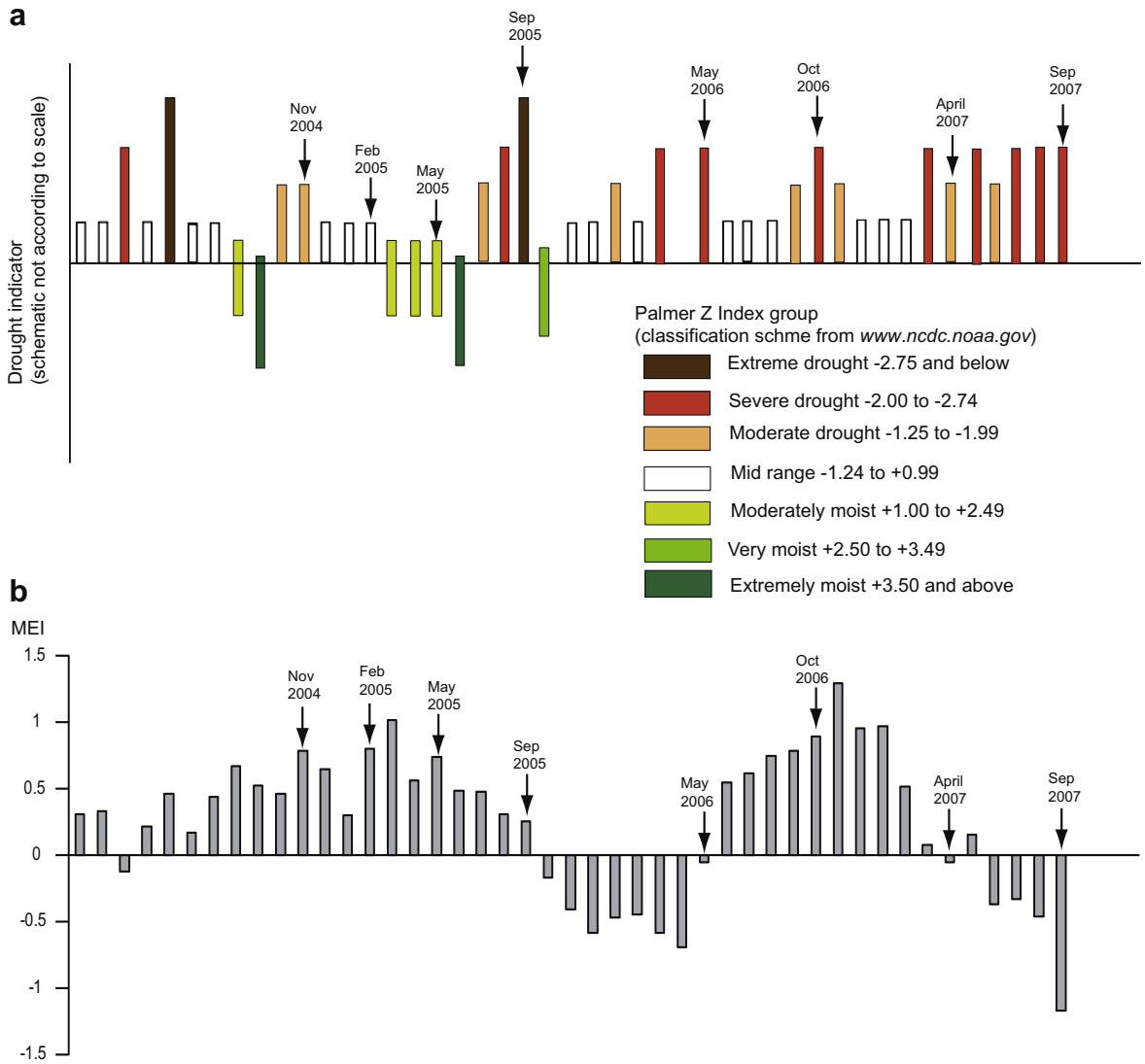

Fig. 7. Variations in monthly ENSO and Palmer Z index (drought indicator) from 2004 to 2007. The sampling periods are labeled by the month and year. (a) Changes in Palmer Z Index from January 2004 to September 2007 at Indian River Lagoon region. Source: http://www.ncdc.noaa.gov/sotc/drought. Color coding scheme is same as used by NOAA. *Note: y* axis is scaled relative to the Palmer Z indicator ranges to emphasize the difference in drought level among different color groups (see the color scheme for bar range). (b) Changes in Multivariate ENSO Index (MEI) from January 2004 to September 2007. Source: http://www.esrl.noaa.gov/psd/enso/mei/table.html.

influenced much by the storm or that any storm-related diagenetic changes in diagenetic reactions were ephemeral (Figs. 4 and 5). Higher resolution sampling following storms would be required to answer the question of whether flushing of reaction products or back reactions dominate post storm diagenetic reactions.

5.3.2. Seasonal variations in SGD

Annual shifts in the seaward boundary of the subterranean estuary could be caused by seasonal variations in precipitation and recharge, which could control the volume of water available for SGD (Michael et al., 2005; Hougham et al., 2008; Santos et al., 2010). The terrestrially derived fraction of SGD should be greatest during periods of elevated precipitation and lowest during periods of diminished precipitation. Terrestrial SGD can increase a few months after highest recharge, responding to the residence time of groundwater in the coastal aquifer (Michael et al., 2005; Charette, 2007). Depending on the relationship between SGD and diagenetic reactions that alter dissolved Fe concentrations in the subterranean estuary, seasonal variations in SGD could influence the magnitude of dissolved Fe fluxes from the subterranean estuary of Indian River Lagoon.

Calculated PET and precipitation vary seasonally over the Indian River Lagoon, with highest precipitation and PET occurring during the summer (June to September) and lowest during the winter (Fig. 6a). Submarine groundwater discharge to Sebastian River, a small gaining stream south of our field area, varies seasonally, but is highest

during dry periods also suggesting a lag occurs between recharge and discharge (Santos et al., 2010). A delay of 5–7 months has been found between precipitation and highest terrestrial SGD at our study site for data collected between 2004 and 2006 (Smith et al., 2008b), but these signals are not reflected in our long-term measurements of Fe, Mn, and Cl concentrations.

5.4. Inter annual precipitation variations and their influence on hydrology and metal flux

Hydrological conditions in a subterranean estuary may vary annually and may be related to climate change (e.g., Anderson and Emanuel, 2008, 2010). During our study period, atmospheric moisture content (as shown by the Palmer Z index) and recharge decrease over three years and reflect moderate drought conditions (Fig. 7a) and negative recharge (Fig. 6b) in 2006 and 2007. Similar drought conditions were also observed on the Florida Gulf coast (Santos et al., 2009a). The landward shift of the freshwater–saltwater boundary occurred between September 2005 and October 2006 sampling period (Fig. 3) reflecting a shift to drier conditions. Rates of precipitation and groundwater recharge were found to change over a 57-year modeling period at barrier islands along the southeastern U.S. coastline (Hatteras Island, North Carolina) in concert with ENSO (Anderson and Emanuel, 2010). In the southeastern US, the ENSO signal propagates through the aquifer with approximately 0–5 month lag (Anderson and Emanuel, 2008, 2010). A similar 5–7 month lag between recharge and discharge was found for the Indian River Lagoon subterranean estuary (Smith et al., 2008b). A weak El Niño year began in September 2006, which would be expected to impact SGD from the Indian River Lagoon subterranean estuary by March–April 2007. The simultaneous timing of drought conditions, the onset of El Niño conditions, and the landward shift of the freshwater–saltwater boundary at the Indian River Lagoon subterranean estuary leads us to hypothesize that annual change in precipitation at our study area is possibly due to ENSO variations, but to prove this link between long-term climate change and variations in SGD and metal fluxes would require longer periods of study.

In addition to changes in the position of the seaward boundary of the subterranean estuary, Fe and Mn distributions showed a systematic change in concentrations during the shift from wet to dry years (Figs. 4 and 5). Dissolution of Fe and Mn oxides and precipitation of Fe-sulfide solid phases are enhanced along the seaward edge of the subterranean estuary because of the sharp changes in salinity and redox conditions there. Consequently, the landward shift of the elevated metal concentration zone likely reflects changes in diagenesis along the seaward edge of the subterranean estuary. Because the Fe-oxide dissolution rate remained approximately constant from 2004 to 2007, elevated Fe concentrations during the landward shift in the seaward boundary of the subterranean estuary do not result from increased reductive dissolution of Fe oxides over the period of decreased discharge. Rather, elevated dissolved Fe concentrations at the boundary probably result from the accumulation of dissolved Fe at the boundary over time as flow rates decreased with diminished offshore hydraulic head. This correspondence between hydrology and trace metal concentrations suggests that not only do changes in inter-annual recharge events affect the position of salinity gradients in subterranean estuaries, these recharge events also affect the spatially averaged magnitude of dissolved metal concentrations. Although we have no nutrient data (e.g., N and P concentrations) corresponding to these metal concentrations, we expect that changes in redox conditions and diagenetic reactions associated with inter-annual precipitation variations would also affect concentrations of these nutrients and their fluxes to subterranean estuaries (e.g., Slomp et al., 1996).

6. CONCLUSION

This study showed the reaction rates of dissolved Fe production and consumption remained approximately constant over the study period, but the dissolved Fe flux from the seepage face (25 m wide in 2004 and 20 m wide in 2007) decreased from 192 to 153 g/yr for a 1-m wide strip of the seepage face. The Fe-oxide reduction reflects OC remineralization at a stoichiometric ratio of 4, and thus the corresponding OC remineralization decreased from 48 to 38 g/yr. Because the Fe-oxide reduction rate did not change much, this inter annual metal flux variation probably is largely a result of the decrease in the size of the subterranean estuary caused by the shift in the position of the freshwater–saltwater boundary resulting from a change in the meteoric recharge to coastal aquifers. Annual aquifer recharge to the unconfined Surficial Aquifer of east-central Florida decreased from about 40 cm/year in 2004 to −10 cm/year in 2007 as a result of a decrease in precipitation by about 1.5 times, although evapotranspiration remained approximately constant. The resulting drought conditions in 2006 and 2007 decreased aquifer recharge and caused the freshwater–saltwater boundary to shift landward by 5 m, decreasing the width of the seepage face. This annual change in precipitation corresponded to a shift from wet La Nina to dry El Niño conditions, but it remains uncertain if SGD and metal fluxes are controlled by ENSO cycles. This study showed that precipitation and recharge of coastal aquifers can control the temporal variations in dissolved Fe flux and associated OC remineralization in subterranean estuaries. Although our study focused on metal and OC reactions, similar changes in other solutes, such as nutrients (N and P) may also be impacted by inter-annual changes in recharge to coastal aquifers. Consequently, estimates of fluxes from subterranean estuaries should consider decadal-scale variations in hydrogeologic characteristics of subterranean estuaries.

ACKNOWLEDGMENTS

This work has been supported by National Science Foundation grant EAR-0403461 (J.B.M.) and EAR-0403515 (J.E.C.). We appreciate the help of Dr. Jennifer Cherrier of Florida A & M University and her graduate student Amanda Dorsett for their assistance with sample collection. We acknowledge Dr. George Kamenev for helping us with ICP-MS analysis. We also acknowledge our editor

Dr. C.J. Daughney and two anonymous reviewers for their critical suggestions to improve this manuscript. Any use of trade, firm, or product names is for descriptive purposes only and does not imply endorsement by the U.S. Government.

APPENDIX A. SUPPLEMENTARY DATA

Supplementary data associated with this article can be found, in the online version, at http://dx.doi.org/10.1016/j.gca.2012.10.055.

REFERENCES

Anderson, Jr., W. P. and Emanuel R. E. (2008) Effect of interannual and interdecadal climate oscillations on groundwater in North Carolina. *Geophys. Res. Lett.* **35**, L23402. http://dx.doi.org/10.1029/2008GL036054.

Anderson W. P. and Emanuel R. E. (2010) Effect of interannual climate oscillations on rates of submarine groundwater discharge. *Water Resour. Res.* **46**, W05503. http://dx.doi.org/10.1029/2009WR008212.

Beck A. J., Cochran J. K. and Sañudo-Wilhelmy S. A. (2010) The distribution and speciation of dissolved trace metals in a shallow subterranean estuary. *Mar. Chem.* **121**, 145–156.

Black P. E. (2007) Revisiting the Thornthwaite and Mather water balance. *J. Am. Water Res. Ass. (JAWRA)* **43**, 1604–1605.

Bokuniewicz H., Pollock M., Blum J. and Wilson R. (2004) Submarine ground water discharge and salt penetration across the sea floor. *Ground Water* **42**, 983–989.

Burnett W. C., Bokuniewicz H., Huettel M., Moore W. S. and Taniguchi M. (2003) Groundwater and pore water inputs to coastal zone. *Biogeochemistry* **66**, 3–33.

Burnett W. C., Wattayakorn G., Taniguchi M., Dulaiova H., Sojisuporn P., Rungsupa S. and Ishitobi T. (2007) Groundwater-derived nutrient inputs to the Upper Gulf of Thailand. *Cont. Shelf Res.* **27**, 176–190.

Cable J. E., Martin J. B. and Jaeger J. (2006) Exonerating Bernoulli? On evaluating the physical and biological processes affecting marine seepage meter measurements. *Limnol. Oceanogr. Meth.* **4**, 172–183.

Cable J. E. and Martin J. B. (2008) In situ evaluation of nearshore marine and fresh pore water transport into Flamengo Bay, Brazil. *Estuar. Coast. Shelf Sci.* **76**, 473–483.

Charette M. A. and Sholkovitz E. R. (2002) Oxidative precipitation of groundwater-derived ferrous iron in the subterranean estuary of a coastal bay. *Geophys. Res. Lett.* **29**(10). http://dx.doi.org/10.1029/2001GLO4512.

Charette M. A., Sholkovitz E. R. and Hansel C. M. (2005) Trace element cycling in a subterranean estuary: Part 1. Geochemistry of the permeable sediments. *Geochim. Cosmochim. Acta* **69**, 2095–2109.

Charette M. A. (2007) Hydrologic forcing of submarine groundwater discharge: Insight from a seasonal study of radium isotopes in a groundwater-dominated salt marsh estuary. *Limnol. Oceanogr.* **52**, 230–239.

Church T. M. (1996) An underground route for the water cycle. *Nature* **380**, 579–580.

Cline J. (1969) Spectrophotometric determination of hydrogen sulphide in natural waters. *Limnol. Oceanogr.* **14**, 454–458.

Cooper H. H. (1959) A hypothesis concerning the dynamic balance of fresh water and salt water in a coastal aquifer. *J. Geophys. Res.* **71**, 461–467.

Dorsett A., Cherrier J., Martin J. B. and Cable J. E. (2011) Assessing hydrologic and biogeochemical controls on pore-water dissolved inorganic carbon cycling in a subterranean estuary: A ^{14}C and ^{13}C mass balance approach. *Mar. Chem.* **127**, 76–89.

Dulaiova H., Burnett W. C., Wattayakorn G. and Sojisuporn P. (2006) Are groundwater inputs into river-dominated areas important? The Chao Phraya River–Gulf of Thailand. *Limnol. Oceanogr.* **51**, 2232–2247.

Elrod V. A., Berelson W. M., Coale K. H. and Johnson K. S. (2004) The flux of iron from continental shelf sediments: A missing source for global budgets. *Geophys. Res. Lett.* **31**, L12307.

Fetter C. W. (2001) *Applied Hydrogeology*, third ed. Prentice Hall, Upper Saddle River, New Jersey, p. 691.

Froelich P. N., Klinkhammer G. P., Bender M. L., Luedtke N. A., Heath G. R., Cullen D. P. D., Hammond D., Hartman B. and Maynard V. (1979) Early oxidation of organic matter in pelagic sediments of the Eastern equatorial Atlantic: Suboxic diagenesis. *Geochim. Cosmochim. Acta* **43**, 1075–1090.

Fung I. Y., Meyn S. K., Tegan I., Doney S. C., John J. G. and Bishop K. B. (2000) Iron supply and demand in the upper ocean. *Global Biogeochem. Cycles* **14**, 281–295.

Glover R. E. (1964) The pattern of fresh-water flow in a coastal aquifer. In *Sea Water in Coastal Aquifers*, vol. 613. U.S. Geol. Surv. Water Supply Pap., pp. 32–35.

Hall G. E. M., Vaive J. E., Beer R. and Hoashi M. (1996) Selective leaches revisited, with emphasis on the amorphous oxyhydroxide phase extraction. *J. Geochem. Explor.* **56**, 59–78.

Hartl K. M. (2006) Facies distribution and hydraulic conductivity of lagoonal sediments in a Holocene transgressive barrier island sequence, Indian River Lagoon, Florida. MS. thesis, University of Florida.

Herzberg A. (1901) Die Wasserversogung eniger Nordseebader. *J. Gasbeleucht. Wasser. (Minich)* **44**, 815–819, and 842–844.

Hougham A. L., Moran S. B., Masterson J. P. and Kelly R. P. (2008) Seasonal changes in submarine groundwater discharge to coastal salt ponds estimated using ^{226}Ra and ^{228}Ra as tracers. *Mar. Chem.* **109**, 268–278.

Hutchins D. A., DiTullio G. R., Zhang Y. and Bruland K. W. (1998) An iron limitation mosaic in the California upwelling regime. *Limnol. Oceanogr.* **43**, 1037–1054.

Lu J., Sun G., McNulty S. G. and Amatya D. M. (2005) A comparison of six potential evapotranspiration methods for regional use in the southeastern United States. *J. Am. Water Res. Ass. (JAWRA)*, 621–633, Paper no. 03175.

Martin J. B., Hartl K. M., Corbett D. R., Swarzenski P. W. and Cable J. E. (2003) A multi-level pore-water sampler for permeable sediments. *J. Sed. Res.* **73**, 128–132.

Martin J. B., Cable J. E., Swarzenski P. W. and Lindenberg M. K. (2004) Enhanced submarine ground water discharge from mixing of porewater and estuarine water. *Ground Water* **42**, 1000–1010.

Martin J. B., Cable J. E., Jaeger J., Hartl K. and Smith C. G. (2006) Thermal and chemical evidence for rapid water exchange across the sediment-water interface by bioirrigation in the Indian River Lagoon, Florida. *Limnol. Oceanogr.* **51**, 1332–1341.

Martin J. B., Cable J. E., Smith C. G., Roy M. and Cherrier J. (2007) Magnitudes of submarine groundwater discharge from marine and terrestrial sources: Indian River Lagoon, Florida. *Water Resour. Res.* **43**. http://dx.doi.org/10.1029/2006WR005266.

Martin J. H. and Fitzwater S. E. (1988) Iron deficiency limits phytoplankton growth in the north-east Pacific Subarctic. *Nature* **331**, 341–343.

Martin J. H., Coale K. H., Johnson K. S., Fitzwater S. E., Gordon R. M., Tanner S. J., Hunter C. N., Elrod V. A., Nowicki J. L.,

Coley, Barber R. T., Lindley S., Watson A. J., Van Scoy K., Law C. S., Liddicoat M. I., Ling R., Stanton T., Stockel J., Collins C., Anderson A., Bidigare R., Ondrusek M., Latasa M., Millero F. J., Lee K., Yao W., Zhang J. Z., Friederich G., Sakamoto C., Chavez F., Buck K., Kolber Z., Greene R., Falkowski P., Chisholm S. W., Hoge F., Swift R., Yungel J., Turner S., Nightingale P., Hatton A., Liss P. and Tindale N. W. () Testing the iron hypothesis in ecosystems of the equatorial Pacific Ocean. *Nature* **371**, 123–129.

McManus J., Berelson W. M., Severmann S., Johnson K. S., Hammond D. E., Roy M. and Coale K. H. (2012) Benthic manganese fluxes along the Oregon–California continental shelf and slope. *Cont. Shelf Res.* **43**, 71–85.

Michael H. A., Mulligan A. E. and Harvey C. F. (2005) Seasonal oscillations in water exchange between aquifers and the coastal ocean. *Nature* **436**, 1145–1148.

Moore W. S. and Church T. M. (1996) Submarine groundwater discharge. *Nature* **382**, 122.

Moore W. S. (1999) The subterranean estuary: A reaction zone of ground water and sea water. *Mar. Chem.* **65**, 111–125.

Moore W. S. (2003) Sources and fluxes of submarine groundwater discharge delineated by radium isotopes. *Biogeochemistry* **66**, 75–93.

Parkhurst D. L. and Appelo C. A. J. (1999) User's Guide to PHREEQC (Version 2)—A computer program for speciation, batch-reaction, one-dimensional transport, and inverse geochemical calculations. *U.S. Geological Survey Water-Resources Investigations Report* **99–4259**, 312.

Roy M., Martin J. B., Cherrier J., Cable J. E. and Smith C. G. (2010) Influence of sea level rise on iron diagenesis in an east Florida subterranean estuary. *Geochim. Cosmochim. Acta* **74**, 5560–5573.

Roy M., Martin J. B., Smith C. G. and Cable J. E. (2011) Reactive-transport modeling of iron diagenesis and associated organic carbon remineralization in a Florida (USA) subterranean estuary. *Earth Planet. Sci. Lett.* **304**, 191–201.

Roy M., Rouxel O., Martin J. B. and Cable J. E. (2012) Iron isotope fractionation in a sulfide-bearing subterranean estuary and its potential influence on oceanic Fe isotope flux. *Chem. Geol.*. http://dx.doi.org/10.1016/j.chemgeo.2012.01.022.

Santos I. R., Dimova N., Peterson R. N., Mwashote B., Chanton J. and Burnett W. C. (2009a) Extended time series measurements of submarine groundwater discharge tracers (^{222}Rn and CH_4) at a coastal site in Florida. *Mar. Chem.* **113**, 137–147.

Santos I. R., Burnett W. C., Chanton J., Dimova N. and Peterson R. N. (2009b) Land or ocean?: Assessing the driving forces of submarine groundwater discharge at a coastal site in the Gulf of Mexico. *J. Geophys. Res.* **114**, C04012.

Santos I. R., Burnett W. C., Dittmar T., Suryaputra I. G. N. A. and Chanton J. (2009c) Tidal pumping drives nutrient and dissolved organic matter dynamics in a Gulf of Mexico subterranean estuary. *Geochim. Cosmochim. Acta* **73**, 1325–1339.

Santos I. R., Peterson R. N., Eyre B. D. and Burnett W. C. (2010) Significant lateral inputs of fresh groundwater into a stratified tropical estuary: Evidence from radon and radium isotopes. *Mar. Chem.* **121**, 37–48.

Scott T. M. (1988) The lithostratigraphy of the Hawthorn Group (Miocene) of Florida. *Florida Geol. Surv. Bull.* **59**, 148.

Severmann S., McManus J., Berelson W. M. and Hammond D. E. (2010) The continental shelf benthic iron flux and its isotope composition. *Geochim. Cosmochim. Acta* **74**, 3984–4004.

Slomp C. P., Van der Gaast S. J. and Van Raaphorst W. (1996) Phosphorus binding by poorly crystalline iron oxides in North Sea sediments. *Mar. Chem.* **52**, 55–73.

Smith N. P. (1987) An introduction to the tides of Florida's Indian River Lagoon. Part I. Water levels. *Florida Sci.* **50**, 49–61.

Smith C. G., Cable J. E. and Martin J. B. (2008a) Episodic high intensity mixing events in a subterranean estuary: Effects of tropical cyclones. *Limnol. Oceanogr.* **53**, 666–674.

Smith C. G., Cable J. E., Martin J. B. and Roy M. (2008b) Evaluating the source and seasonality of submarine groundwater discharge using a radon-222 pore water transport model. *Earth Planet. Sci. Lett.* **273**, 312–322.

Snyder M., Taillefert M. and Ruppel C. (2004) Redox zonation at the saline-influenced boundaries of a permeable surficial aquifer: Effects of physical forcing on the biogeochemical cycling of iron and manganese. *J. Hydrol.* **296**, 164–178.

Spiteri C., Regnier P., Slomp C. P. and Charette M. A. (2006) PH dependent iron oxide precipitation in a subterranean estuary. *J. Geochem. Explor.* **88**, 399–403.

Spiteri C., Slomp C. P., Charette M. A., Tuncay K. and Meile C. (2008) Flow and nutrient dynamics in a subterranean estuary (Waquoit Bay, MA, USA): Field data and reactive transport modeling. *Geochim. Cosmochim. Acta* **72**, 3398–3412.

Sunda W. G., Barber R. T. and Huntsman S. A. (1981) Phytoplankton growth in nutrient rich seawater: Importance of copper–manganese cellular interactions. *J. Mar. Res.* **39**, 567–586.

Taniguchi M., Ishitobi T. and Saeki K. (2003) Evaluations of time-space distributions of submarine ground water discharge. *Ground Water* **43**, 336–342.

Testa J. M., Charette M. A., Sholkovitz E. R., Allen M. C., Rago A. and Herbold C. W. (2002) Dissolved iron cycling in the subterranean estuary of a coastal bay: Waquoit Bay, Massachusetts. *Biol. Bull.* **203**, 255–256.

Thornthwaite C. W. and Mather J. R. (1957) Instructions and tables for the computing potential evapotranspiration and the water balance. In *Publications in Climatology*, vol. X(3), p. 311. Publications in Climatology. John Hopkins University.

Windom H. L., Moore W. S., Niencheski L. F. H. and Jahnke R. A. (2006) Submarine groundwater discharge: A large, previously unrecognized source of dissolved iron to the South Atlantic Ocean. *Mar. Chem.* **102**, 252–266.

Associate editor: Christopher John Daughney